ELSEVIER

Surface Science 344 (1995) 251–257

surface science

Binding and diffusion of a Si adatom around type B steps on Si(001) c(4 × 2)

Jun Wang [a], D.A. Drabold [b], A. Rockett [a,*]

[a] *Materials Research Laboratory and the Department of Materials Science and Engineering, University of Illinois, 1101 West Springfield Avenue, Urbana IL61801, USA*

[b] *Department of Physics and Astronomy, Ohio University, Athens, OH 45701, USA*

Received 26 January 1995; accepted for publication 11 July 1995

Abstract

Maps of the binding energy of an adatom on Si(001) c(4 × 2) around the nonbonded and bonded type B surface steps are presented. The results suggest that the nonbonded type B step should accumulate adatoms rapidly both from above and below. The energy barrier to cross the nonbonded step is ~0.2 eV greater than for diffusion on the flat surface. The binding sites along the nonbonded step edge are similar to those on the flat surface but are paired and connected by a low-energy diffusion pathway that may facilitate formation of dimers along the step edge. The bonded step attracts adatoms ~0.5 ± 0.2 eV more strongly than any other site on the surface. However, these sites are relatively inaccessible due to surrounding high energy barriers. Based on the results, the upper side of the bonded step should be repulsive to adatoms. The diffusion barrier for adatoms approaching the step rises and the binding sites become less favorable there. Hence, growth of the bonded step is probably much slower than the nonbonded step, which explains its observed predominance on Si(001) surfaces.

Keywords: Atomistic dynamics; Density functional calculations; Silicon

1. Introduction

Microelectronic device applications require increasingly short range changes in the properties of their constituent materials, in some cases over distances of one atomic layer. Great progress in forming such abrupt junctions has been achieved. However, further progress will require a more detailed understanding of atom dynamics. Of the technologically important materials and surfaces, Si(001) is by far the most widely used. The basic reconstruction of this surface is dimerization leading to a 2 × 1 structure. However, tilt of the dimers has been predicted to yield a c(4 × 2) structure [1]. Studies of Si(001) have given an excellent picture of the static surface [2–5]. However, to understand adatom dynamics it is necessary to follow the motion of individual adatoms as they diffuse. Unfortunately, to date it has been impossible to observe the motion of single adatoms directly. To study these indirectly, computer simulations based on the Monte Carlo [6–8] or molecular statics [9–11] approaches have been developed. Both experimental and theoretical studies of the structure of Si(001) c(4 × 2) grown by molecular beam epitaxy (MBE) suggest that under many conditions the morphology is dominated by attachment of atoms to the three types of surface steps (type A, bonded type B, and

* Corresponding author.

SSDI 0039-6028(95)00806-3

nonbonded type B [12]). For example, step-evolution analysis [8], Monte Carlo (MC) simulations [7,8], and density functional theory [13] have suggested that the type A step presents no significant barrier to adatom diffusion and may bind adatoms weakly to the step. Furthermore, it was suggested [7] that the morphology of surfaces during growth is primarily determined by the interaction of adatoms with type A steps. In this paper, we extend our previous work on adatom dynamics around the type A step [13] to consider the properties of the adatom around the two type B steps of the Si(001) surface based on density functional theory.

2. Simulation method

The calculations reported here used an approach developed by Sankey and coworkers and described in detail elsewhere [13–16]. The calculation was carried out under the local density approximation and used non-local norm-conserving pseudopotentials and a pseudoatomic wave function basis set that eliminates the requirement of periodic boundary conditions. While the method does not provide a self-consistent solution of the density functional equations for the system, the results have been shown to provide an excellent description of a variety of systems including Si surface reconstructions [17–19].

Theoretical studies of the type B surface steps to date have focused on the step structure and stability [1,12]. The two possible type B steps are shown schematically in Fig. 1. The terms bonded and nonbonded refer to the attachment of a row of dimerized atoms to the bottom edge of the step or the absence of this row, respectively [12]. The tilting of the dimers on both the upper and lower terraces increases the number of possible configurations of the step from two to eight. Out of the eight possible configurations, Boguslawski et al. [1] found that the ground state of the type B steps consists of a $p(2\times2)$ tilted dimer reconstruction near the upper terrace edge and a $c(4\times2)$ tilted dimer reconstruction domain on the lower terrace. The dimers attached to the edge of the bonded B

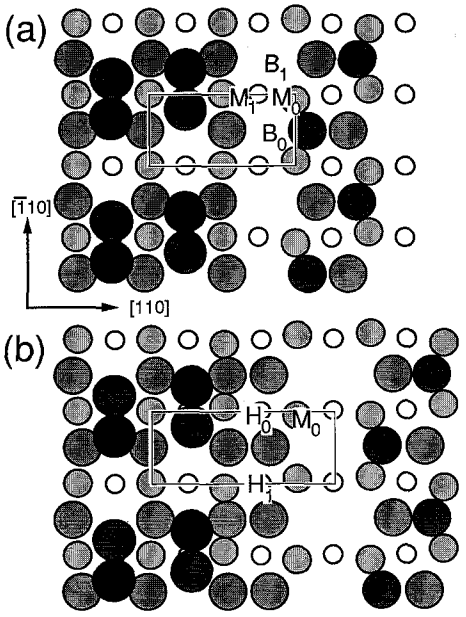

Fig. 1. Schematic diagrams of the Si(001) $c(4\times2)$ simulation cells used here. Darker shading and larger diameters indicate atoms closer to the surface. Areas of the energy maps (rectangles) of (a) the nonbonded type B and (b) the bonded type B steps are also indicated. The minimum energy positions, long bridge sites in the channel and the four-fold sites on top of the dimer row are labeled M, B and H, respectively. Subscripts distinguish sites of the same local symmetry but different longer range symmetry.

step are stretched so that they are less tilted and their bond lengths are longer than for flat surface dimers. The bonded type B steps also have a long range strain field associated with them [20]. Poon et al. [20] showed that a system with more than 1000 atoms is needed to take the strain field of this step into consideration accurately. This is impossible with density functional theories such as we employ here. However, the forces acting on an adatom are largely determined by the local atomic geometry. While the long range strain term affects the total energy of the step, the effect of an adatom on this field, and thus the relative change in its binding energy, is a local phenomenon.

Top views of the simulation cells used in this study are given in Fig. 1. The upper terraces consisted of dimer rows two dimers in length and perpendicular to the step edges. Periodic boundary conditions were used around the edges of the cell.

This causes the long range strain field of the system to cancel out. The thickness of the slab is six atomic layers on the lower terrace. Larger simulation cells were used to check the convergence of the step structure and formation energy. The simulation cell used in this study yielded step formation energies, dimer tilt angles, and bond lengths within $\pm 10\%$ of values obtained for larger unit cells, which should be adequate for purposes of this study. All calculations indicate that the stable structure of the type B step consists of $p(2\times 2)$ and $c(4\times 2)$ reconstruction domains on the upper and lower terraces, respectively, in agreement with the results of Boguslawski et al. [1].

Energy maps as a function of the position of a Si adatom were constructed for the two type B steps using a method described previously [13]. The areas mapped for each step are indicated in Fig. 1. The coordinates of mesh points were determined by averaging the positions of atoms along a given mesh direction for each of the top three atomic layers. The mesh was positioned to yield points with the highest average symmetry with respect to the atoms. Perpendicular to the step edge there were nine mesh points for the nonbonded step and eleven for the bonded step. There were five points along the step edge direction for both maps.

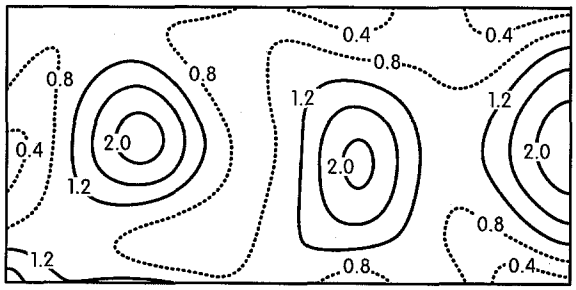

(a)

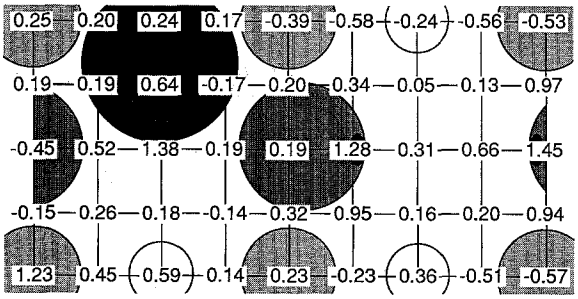

(b)

Fig. 2. Energy maps of a Si adatom around the nonbonded type B step. (a) Contour energy map for the surface with a contour interval of 0.4 eV. The zero energy for the contour map was the energy of the most favorable binding sites on the flat surface. Dashed lines indicate contours with energy ≤ 0.8 eV while solid lines represent contours of higher energies. (b) The calculated numerical values referenced to the energy at the saddle point for diffusion on the flat surface. Approximate surface atom positions before relaxation due to the presence of the adatom are shown for reference. Atoms are shown larger and darker when closer to the surface. Dangling bonds are indicated by ellipses.

3. Results

Surface energy maps for the nonbonded and bonded type B steps are shown in Fig. 2 and Fig. 3, respectively. The maps for both types of steps covered only the lower side of one of the tilted dimers in the upper terrace. This side of the dimers should be more favorable for diffusion based on the previous studies of the type A step and flat surface [13]. The maps started at the middle of the upper terraces. The two-dimer-wide upper terraces were too narrow to converge to the flat surface result at all points. Unfortunately, larger terraces were found to be computationally impractical for generating full energy maps. Convergence to the flat surface behavior was found for the channel between dimer rows on the upper terraces of both simulation cells but the dimer top sites were destabilized by the presence of the steps and hence were less favorable than on a flat surface at all simulated points. The destabilization behavior should be correct near the step edges (in spite of the small simulation cells) and results from the local strain fields generated by the steps. The principal question is how far this effect extends into the terraces before converging to the flat surface behavior. The comparison is further complicated by the difference in symmetry between the simulation cells, i.e. $p(2\times 2)$ for the upper terrace near a step and $c(4\times 2)$ for the flat surface, so exact convergence is not expected in any case. On the basis of the simulations to date, convergence

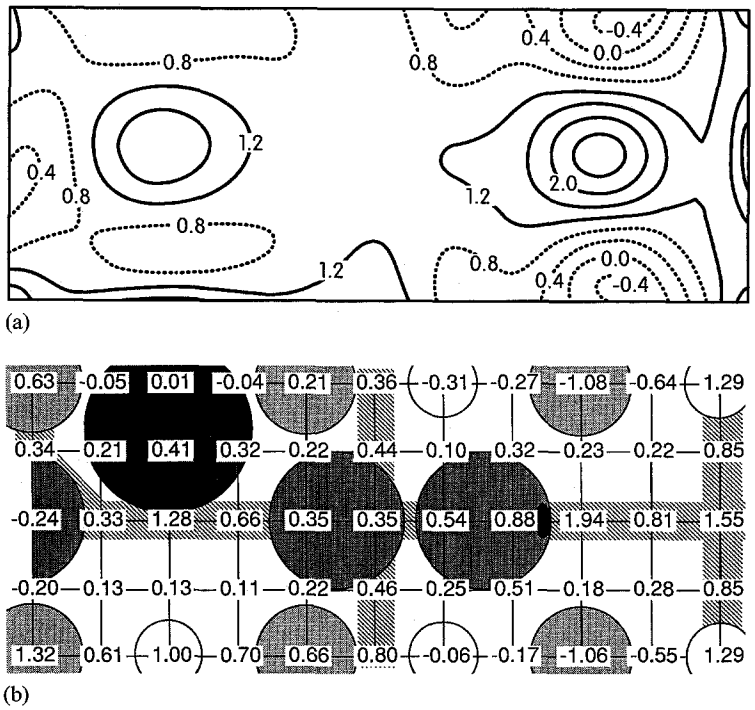

Fig. 3. Energy maps of a Si adatom around the bonded type B step. (a) A contour energy map with contours as in Fig. 2a. (b) The calculated numerical values as in Fig. 2b. Cross hatched bands in the background indicate the high energy "walls" (with energies ≥ 0.3 eV above the energy required for diffusion on the flat surface) which develop around this step.

would probably occur after only another one or two additional surface lattice spacings.

On the lower terrace the energy maps terminated along the atoms underlying the dimer row nearest the step in the lower terrace for the nonbonded step map and along the channel center between dimer rows for the bonded step map (see Fig. 1). Differences from the flat surface behavior around the simulation cell edges for the nonbonded step calculation probably resulted from the small simulation cells, while differences for the bonded step are almost certainly due to intrinsic changes in the energy surface structure.

3.1. *The nonbonded step*

We begin detailed discussion of the results with the nonbonded step. The most favorable binding sites are the two-fold stacking fault sites between dimers along the side of the first dimer row on the lower terrace (M_0 in Fig. 1a) and between the dangling bonds of the atoms of the step edge adjacent to the end of the upper terrace dimer row (M_1 in Fig. 1a). These two sites bound atoms with the same strength as did the minimum energy sites on flat surfaces (which were of the same general type). The two-fold site between step edge atoms adjacent to the interdimer channels of the upper terrace (halfway between M_1 sites) was less stable by ~ 0.35 eV relative to the sites adjacent to the upper terrace dimer rows (M_1), apparently because the distance to the dangling bonds to which the adatom binds was longer. Unlike the flat surface result where the M_0 sites are separated by a high energy barrier in the channel between dimer rows, the M_0 and M_1 sites are connected by a low-energy-barrier pathway. Thus, transfer of atoms from the last dimer row on the lower terrace to the step edge is rapid and reversible.

The long bridge lattice sites between the step edge atoms and the atoms in the adjacent dimer row (site B_0 in Fig. 1a) are not attractive to ada-

toms and are the saddle points for diffusion along the channel near the step edge. The barrier is high enough that adatoms are more likely to diffuse along top of the first dimer row adjacent to the step rather than staying near the step edge. This is in contrast to results for this step using empirical potentials [9,21] that suggest a strong binding to these lattice sites and the presence of a deep diffusion channel along the step edge. The other (inequivalent) long bridge site (B_1 in Fig. 1a) in the trench area was not covered by the map but was calculated separately for comparison. This site binds the adatom $\sim$0.4 eV more strongly than site B_0 but still lies 0.5 eV above the M_0 and M_1 energies.

The adatom can cross the nonbonded type B step either over the top of the dimer row ending the upper terrace or around the lower end of the edge dimer. These pathways are similar to the equivalent pathways on the flat surface but are closer in activation energy. An extra energy of $<0.2\pm0.1$ eV above that needed to diffuse on the flat surface is required for the adatom to cross the step along either path. Diffusion across the step deposits the adatom in the M_1 sites from which transfer to the M_0 sites is rapid. Diffusion along the step edge can then occur along the adjacent dimer row as on the flat surface. The paired binding sites along the nonbonded type B step (M_0 and M_1) may increase the probability of adatoms meeting and rearranging to form a dimer along the step edge. Furthermore, the step edge can collect adatoms relatively rapidly from above and from the dimer row running along the edge below. The increased area from which atoms can be collected, along with the paired binding sites at the step edge, should make growth of the nonbonded type B step relatively rapid. Furthermore, the relatively rapid exchange of atoms across the step and with the dimer row adjacent to the lower terrace edge should permit rapid diffusion along the edge. This would increase the chances of adatoms meeting along the edge, and would result in lateral growth of the nonbonded type B step. Finally, we note that the relatively large supply of adatoms to the dimer row adjacent to the step edge may permit formation of dimers on that row in addition to along the step edge, consistent with experimental results.

3.2. The bonded step

The behavior of the adatom around the bonded type B step is quite different from that of the nonbonded step because of the 0.013 nm displacement of the bonded dimers toward the step edge and displacement of the last dimer in the upper terrace by 0.054 nm in the direction of the bonded dimer. The most dramatic effect of these displacements is the formation of high energy barriers to diffusion (see Fig. 3b) along a line through the bonded dimer and along the channel between the bonded dimers and the adjacent dimer row on the lower terrace. The effect of these energy walls is to break the surface near the bonded step edge into small binding pockets separated by high barriers. While the calculation did not converge to the flat surface behavior on the lower terrace, the high energy barrier between the next dimer row and the step edge suggests that transfer of atoms from the lower terrace to the step edge would be extremely slow. Hence, the termination of the simulation at this point should not be significant to the general interpretation of the results.

The two-fold sites between the dangling bonds of the bonded dimer row (M_0 in Fig. 1b) are similar to the most favorable sites on the flat surface and around other steps but are much more strongly bound (by 0.5 eV!). On this type of site, three bonds form between the adatom and the substrate, one to each of the dimer dangling bonds and one back bond to the second layer atom. We suggest three reasons for the increased binding at these sites. First, the displacement of the bonded dimer on the lower terrace exposes the second layer atom. That makes formation of the back bond easier. The distortion of the bonds to the second layer atoms also enhances the strength of the back bond. Second, the tilt of the bonded dimers is reduced relative to those on the flat surface. This decreases the pairing of electrons in the dangling bonds and enhances the bonding to the adatom. Third, because the dimers along the step edge have only one dangling bond, the π-bonded chains that stabi-

lize dimer rows on flat surfaces are insignificant and thus need not be disrupted to form bonds to the adatom along the bonded dimer row.

While the M_0 sites along the bonded dimers are much more attractive to adatoms, all other potential binding sites around the step edge are weakened. The two-fold sites along the dimer rows of the upper terrace are less strong near the step edge, suggesting that the step will tend to repel adatoms from above. The normal diffusion pathway across the dimer tops on the flat surface is also disrupted near the step edge. Both of these effects are consistent with the presence of a large tensile strain in the upper terrace edge that moves the atoms farther apart. On the lower terrace, the strain in the bonded dimer reduces the ability of the adatom to bond there which results in an increase in the energy barrier for crossing the dimer row. Finally, the formation of a high energy barrier in the channel between the bonded dimers and the adjacent dimer row on the lower terrace is due to tensile strain increasing the channel width.

The modified binding site energies and the formation of energy barriers to diffusion may make supply of adatoms to the bonded type B step relatively slow. However, once an adatom reaches the step edge it should be highly stable there. This behavior should make the mechanism of growth of the type B step quite temperature dependent. We note, however, that because the type B step is observed to grow much faster than the type A step on Si(001) c(4 × 2), it must be possible for adatoms to reach the bonded step edge. There are two possible explanations for the supply of atoms to the edge in spite of the energy barriers calculated here. First, the barriers may not be as large as proposed here. This must be considered possible both because density functional theories tend to overestimate bond strengths significantly and because with a surface energy map calculated on the basis of a uniform grid it is possible to miss the minimum energy sites slightly. Of these explanations, the former seems more likely as missing the minimum energy pathway can only account for perhaps 0.1 eV of error. The second and most likely explanation for the rapid growth of the type B step compared to the type A step is that an exchange mechanism such as was suggested by Metiu et al. [8] for the type A step occurs along the bonded type B edge. The very high energies for diffusion and the large surface strain fields around the step make such diffusion pathways likely.

4. Conclusions

The energy map results presented here suggest that the nonbonded type B step should accumulate adatoms rapidly both from above and below which would convert it to the bonded type step. The binding sites along the edge of the nonbonded step are similar to those on flat surfaces but are paired and connected by a low-energy diffusion pathway. Growth of the bonded step is probably much slower, which explains its predominance on the surfaces observed by scanning tunneling microscopy. Although the bonded step attracts adatoms much more strongly than any other point on the surface, these sites are relatively inaccessible due to high energy barriers present surrounding the sites. The upper side of the bonded step is likely to be repulsive to adatoms both because the diffusion barrier for approaching the step rises and because the binding sites become less stable there.

Acknowledgements

A.R. and J.W. gratefully acknowledge the support of the Department of Energy under contract DEFG02-91ER45439. D.A.D. acknowledges partial support from NSF under contract DMR 93-22412.

References

[1] See P. Boguslawski, Q.-M. Zhang, Z. Zhang and J. Bernholç, Phys. Rev. Lett. 72 (1994) 3694; P. Boguslawski, Q.-M. Zhang, Z. Zhang, C. Roland and J. Bernholç, Mater. Sci. Eng. B, in press.

[2] M.J. Bronikowski, Y. Wang and R.J. Hamers, Phys. Rev. B 48 (1993) 12 361.

[3] K. Sugihara, A. Sakai, Y. Kato, Y. Akama and N. Shoda, J. Vac. Sci. Technol. B 9 (1991) 707.

[4] D.G. Cahill and R.J. Hamers, J. Vac. Sci. Technol. B 9 (1991) 564.
[5] See Y.W. Mo, J. Kleiner, M.B. Webb and M.G. Lagally, Surf. Sci. 268 (1992) 275, and references therein; B.S. Swartzentruber, Y.W. Mo and M.G. Lagally, Phys. Rev. Lett. 66 (1991) 1998.
[6] A. Rockett, Surf. Sci. 227 (1990) 208.
[7] A. Rockett, Surf. Sci. 312 (1994) 201.
[8] See Zhen-Yu Zhang, Yan-Ten Lu and H. Metiu, Surf. Sci. 248 (1991) L250; Phys. Rev. B 46 (1992) 1917, and references therein.
[9] See, for example, C. Roland and G.H. Gilmer, Phys. Rev. Lett. 67 (1991) 3188.
[10] F. Stillinger and T. Weber, Phys. Rev. B 31 (1985) 5262.
[11] Surface structure calculations for Si(001) may be found in, for example, F.S. Khan and J.Q. Broughton, Phys. Rev. B 39 (1989) 3688 or Z. Zhu, N. Shima and M. Tsukada, Phys. Rev. B 40 (1989) 11 868.
[12] D. Chadi, Phys. Rev. Lett. 59 (1987) 1691.
[13] J. Wang, D.A. Drabold and A. Rockett, Appl. Phys. Lett. 66 (1995) 1954.
[14] O.F. Sankey and D.J. Niklewski, Phys. Rev. B 40 (1989) 3979.
[15] O.F. Sankey, D.A. Drabold and G.B. Adams, Bull. Am. Phys. Soc. 36 (1991) 924.
[16] O.F. Sankey, D.J. Niklewski and D.A. Drabold, Phys. Rev. B 41 (1990) 12 750.
[17] G.B. Adams and O.F. Sankey, Phys. Rev. Lett. 67 (1991) 867.
[18] G.B. Adams and O.F. Sankey, J. Vac. Sci. Technol. A 10 (1992) 2046.
[19] S.H. Yang, D.A. Drabold and J.B. Adams, Phys. Rev. B 48 (1993) 5261.
[20] Tze Wing Poon, S. Yip, P.S. Ho and F.F. Abraham, Phys. Rev. Lett. 65 (1990) 2161; Phys. Rev. B 45 (1992) 3521.
[21] J. Wang and A. Rockett, unpublished.